Available online at www.sciencedirect.com
ScienceDirect
Physica B 403 (2008) 1170–1172
PHYSICA B
www.elsevier.com/locate/physb

Emergence of the nodal portion of the Fermi surface due to the reduction process in the electron-doped cuprates

P. Richard[a,*], M. Neupane[a], Y.-M. Xu[a], P. Fournier[b], S. Li[c], Pengcheng Dai[c,d], Z. Wang[a], H. Ding[a]

[a]*Department of Physics, Boston College, Chestnut Hill, MA 02467, USA*
[b]*Département de Physique, Université de Sherbrooke, Que., Canada J1K 2R1*
[c]*Department of Physics and Astronomy, The University of Tennessee, Knoxville, TN 37996, USA*
[d]*Neutron Scattering Sciences Division, Oak Ridge National Laboratory, Oak Ridge, TN 37831, USA*

Abstract

We have performed a systematic angle-resolved photoemission study of as-grown (AG) and oxygen-reduced $Pr_{2-x}Ce_xCuO_4$ and $Pr_{1-x}La_xCe_xCuO_4$ electron-doped cuprates. Our results indicate that the nodal region of the Fermi surface, which is suppressed in the AG samples, emerges in the reduced samples due to the suppression of the long-range antiferromagnetic order.

PACS: 74.72.Jt; 74.25.Jb; 74.62.Dh; 79.60.−i

Keywords: Cuprates; Electron doped; ARPES; Superconductivity; Reduction process

1. Introduction

Since the discovery of the so-called T′ electron-doped superconductors $RE_{2-x}Ce_xCuO_4$ and $RE_{1-x}LaCe_xCuO_4$ (RE = (Pr, Nd, Sm, Eu)), the understanding of the reduction process necessary to achieve superconductivity in these materials has attracted much attention. Even at optimal Ce concentration, the as-grown (AG) samples become superconductors only after the removal of a tiny amount of oxygen (~1%) following a post-annealing process [1–4]. The actual debate on the microscopic origin of the reduction process and how it can modify drastically the transport properties [5] calls for a better understanding of the electronic structure of these materials and especially on the changes introduced by the reduction process. Particularly, the suppression of the long-range antiferromagnetic (AF) order after the reduction process [6,7] suggests that a special attention must be devoted to the nodal portions of the Fermi surface around $(\pm\pi/2, \pm\pi/2)$.

2. Experiment, results and discussion

High-quality $Pr_{1.85}Ce_{0.15}CuO_4$ and $Pr_{0.88}LaCe_{0.12}CuO_4$ single crystals have been grown by the flux and floating zone techniques, respectively. Some nonsuperconducting AG samples have been annealed as described in Refs. [8,9] and exhibit superconducting transitions around 24 K. The samples have been studied by ARPES using the PGM and U1-NIM beamlines of the Synchrotron Radiation Center (Stoughton, WI) with 73.5 eV photons. The data have been recorded at 40 K using a Scienta SES-2002 analyzer with a 30 meV energy resolution. The samples have been cleaved *in situ* in a vacuum better than 10^{-10} Torr. Although this letter focuses on the data obtained on $Pr_{2-x}Ce_xCuO_4$, similar results have been obtained for the $Pr_{1-x}LaCe_xCuO_4$ samples.

More than any other parameter, the suppression of the long-range AF order following the reduction process has significant impact on the ARPES spectra. We compare in Figs. 1a and b, respectively, the band dispersion of the reduced and AG samples slightly away from the AF zone boundary, as indicated in the inset of Fig. 1a. In addition

*Corresponding author. Tel.: +1 617 552 6882; fax: +1 617 552 8478.
E-mail address: richarpi@bc.edu (P. Richard).

0921-4526/$ - see front matter © 2007 Elsevier B.V. All rights reserved.
doi:10.1016/j.physb.2007.10.283

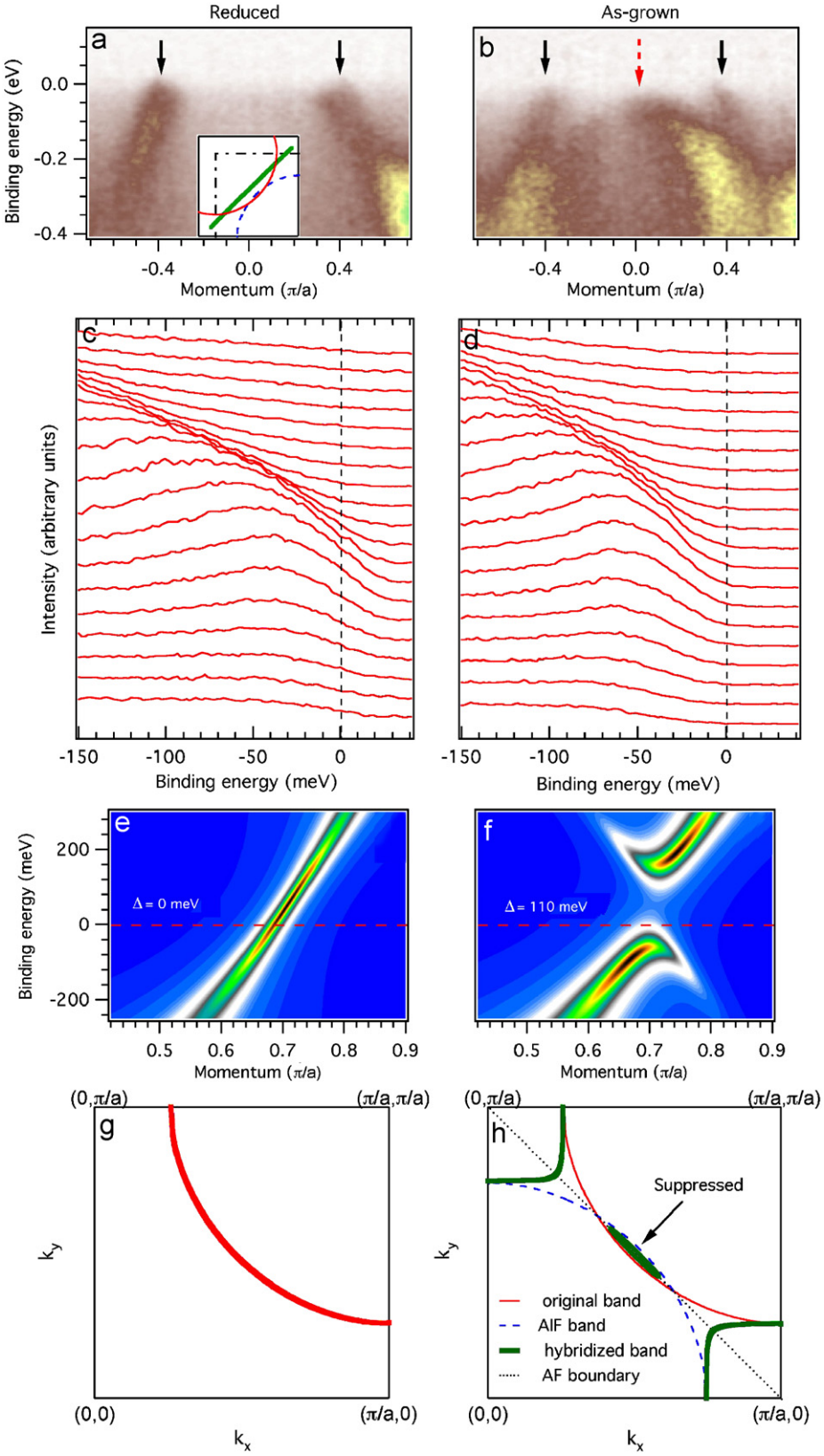

Fig. 1. (a) and (b) ARPES spectra obtained corresponding to the k location given by a thick line in the inset of panel (a), in which the thin solid, the dashed and the dashed and dotted line correspond to the original band, AIF band and Brillouin zone boundary, respectively. The solid and dashed arrows refer to features associated with the original and AIF bands, respectively. (c) and (d) EDC obtained along the nodal direction. (e) and (f) Simulations of the nodal spectra using Δ size AF hybridization gaps (see the text). (g) and (h) Schematic FS.

to the main band, which is identified by solid arrows, the spectra of the AG sample exhibit additional features (dashed arrows) associated with the AF induced folded (AIF) band.

We now ask the question: how the presence of an AIF band can affect the FS and the transport properties. Since they have the same symmetries, the main and AIF bands are expected to hybridize and open a gap everywhere they cross. The momentum (k) locations of these crossings coincide with the magnetic zone boundary and their energy locations depend on the k location on the magnetic zone boundary. These crossings occur slightly above the Fermi energy (E_F) for k located between the hot spots, which are defined as the k locations where the main and AIF bands cross precisely at E_F. Unlike the lower hybridized band, the upper hybridized band never crosses E_F along the nodal direction, and thus cannot be observed by low-temperature ARPES. As the hybridization gap increases, the top of lower hybridized band is pushed down and is eventually gapped out when the hybridization becomes strong enough.

In order to check this scenario, we investigated the band dispersion of the reduced and AG samples and the corresponding energy distribution curves (EDCs) are given in Figs. 1c and d, respectively. In addition to a clear leading edge shift as compared with the reduced sample EDCs, the EDCs of the AG sample exhibit a bending back typical of a hybridization, as confirmed by simple simulations of the nodal spectra in the presence of an AF hybridization gap. Using an effective tight-binding model with parameters obtained from the fit of the underlying FS ($E - 0.05 = -0.55[\cos(k_x) + \cos(k_y)] + 0.32\cos(k_x)\cos(k_y)$), as well as with a proper linewidth, we can simulate qualitatively the nodal spectra of reduced and AG samples by introducing a 0 meV (Fig. 1e) and a 110 meV (Fig. 1f) hybridization gap, respectively.

The first quadrant of the schematic FS of the reduced and AG samples resulting from the AF hybridization scenario is shown in Figs. 1g and h, respectively. While the FS of the reduced sample has large holelike pocket FSs centered at $X(\pi,\pi)$ points, the FS of the AG samples is formed by small electronlike pocket FSs centered at $M(0,\pi)$ points and small holelike pocket FSs centered at $(\pi/2,\pi/2)$. However, as previously shown, the latter is strongly suppressed. The proposed topology of the FS is in good agreement with recent Hall coefficient measurements [5], which suggest the delocalization of holelike carriers after the reduction process. Even though it is not possible at this stage to establish a direct connection between Cooper pairing in cuprates and the presence of the nodal portion of the FS, our results suggest that its presence may play an important role in the mechanism of high-T_c superconductivity.

3. Summary

In summary, our systematic ARPES comparison of the nodal properties of the reduced and AG samples indicates in the latter the presence of a nodal leading edge gap induced by AF hybridization. After the reduction process, our results show that the long-range AF order is suppressed and, as a consequence, no nodal leading edge gap is observed.

Acknowledgments

We are indebted to A.-M.S. Tremblay and D. Sénéchal for useful discussions. We acknowledge support from NSF DMR-0353108, DMR-0645461 (ICAM), DOE DEFG02-99ER45747 and DE-FG02-05ER46202. This work is based upon research conducted at the Synchrotron Radiation Center supported by NSF DMR-0537588. P.F. acknowledges the support of NSERC (Canada), FQRNT (Québec), CFI and CIAR.

References

[1] E. Moran, et al., Physica C 160 (1989) 30.
[2] J.S. Kim, D.R. Gaskell, Physica C 209 (1993) 381.
[3] E. Wang, et al., Phys. Rev. B 41 (1990) 6582.
[4] K. Susuki, et al., Physica C 166 (1990) 357.
[5] J. Gauthier, et al., Phys. Rev. B 75 (2007) 024424.
[6] P. Richard, et al., Phys. Rev. B 72 (2005) 184514.
[7] P. Dai, et al., Phys. Rev. B 71 (2005) 100502.
[8] P. Richard, et al., Phys. Rev. B 70 (2004) 064513.
[9] H.J. Kang, et al., Natur. Materials 6 (2007) 224.